

Intersystem Crossing and Triplet Dynamics in an Fe(II) N-Heterocyclic Carbene Photosensitizer

J. Patrick Zobel,^{*,†} Olga S. Bokareva,[‡] Christoph Wölper,[¶] Peter Zimmer,[§]
Matthias Bauer,[§] and Leticia González^{*,†,||}

[†]*Institute of Theoretical Chemistry, Faculty of Chemistry, University of Vienna,
Währingerstr. 19, 1090 Vienna, Austria*

[‡]*Institute of Physics, Rostock University, Albert Einstein Straße 23-24, 18059 Rostock,
Germany*

[¶]*Department for X-Ray Diffraction, Inorganic Chemistry, University of Duisburg-Essen,
Universitätsstraße 7, D-45117 Essen, Germany*

[§]*Faculty of Science, Chemistry Department and Center for Sustainable Systems Design
(CSSD), Paderborn University, Warburger Str. 100, 33098 Paderborn, Germany*

^{||}*Vienna Research Platform on Accelerating Photoreaction Discovery, University of Vienna,
Währingerstr. 19, 1090 Vienna, Austria*

E-mail: patrick.zobel@univie.ac.at; leticia.gonzalez@univie.ac.at

Supporting Information

This document contains experimental data (1H-NMR, IR, optical absorption spectrum, X-RAY), Cartesian coordinates of the FC geometry, density-of-states for the LC-BLYP/6-31G* calculations in terms of spin-adiabatic states, the characterization of the excited states at the FC geometry, the list of normal modes used in the LVC model, and videos in gif format showing the charge flow during the dynamics. See the following Table of Contents.

Contents

Supporting Information	S1
S1 Experimental Data	S4
S1.1 Analytical Data	S4
S1.2 Optical Absorption Spectrum of [Fe ^{II} (tpy)(pyz–NHC)](PF ₆) ₂	S6
S1.3 Details of Single Crystal Structure Analysis	S6
S2 Ground-State Equilibrium Geometry	S20
S3 Density of States in the Wigner Ensemble	S22
S4 Excited States at the FC Geometry	S24
S5 Normal Modes in LVC Model	S26
S6 Charge Flow During the Dynamics	S30

List of Tables

S1	Crystal Structure Data.	S8
S2	Atomic coordinates and isotropic displacement parameters	S10
S3	Ground-state geometry optimization	S20
S4	State characterization at the FC geometry	S25
S5	Normal modes excluded in the LVC model.	S26

List of Figures

S1	^1H -NMR spectrum.	S4
S2	ESI mass spectrum.	S5
S3	Experimental optical absorption spectrum of $[\text{Fe}^{\text{II}}(\text{tpy})(\text{pyz}-\text{NHC})](\text{PF}_6)_2$ in MeCN.	S6
S4	Crystal structure of $[\text{Fe}^{\text{II}}(\text{tpy})(\text{pyz}-\text{NHC})](\text{PF}_6)_2$	S7
S5	Singlet and triplet density of states	S23

S1 Experimental Data

S1.1 Analytical Data

¹H NMR: NMR spectra were recorded with a Bruker Avance 500 (¹H, 500.1 MHz; ¹³C, 125.8 MHz) in acetone-d6.

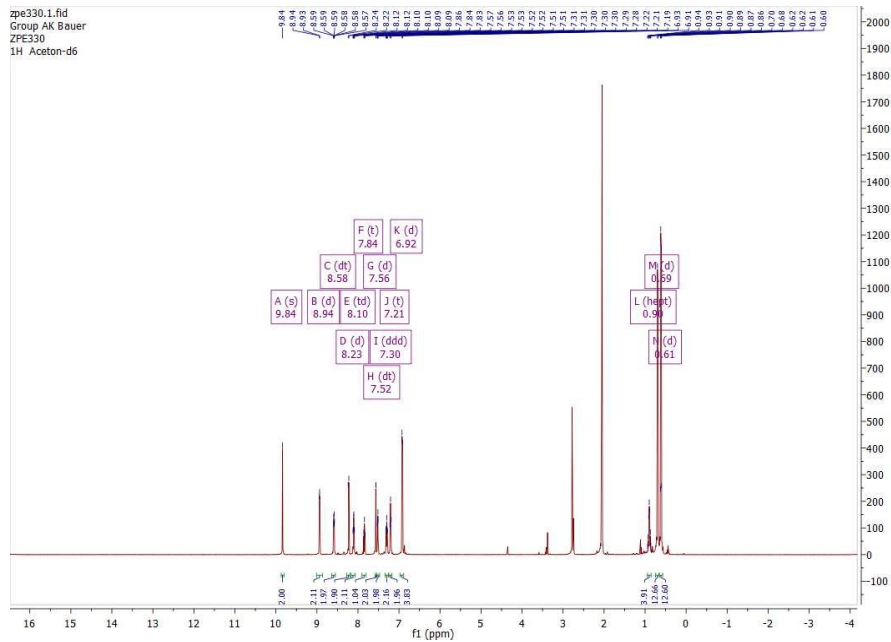


Figure S1: ¹H-NMR spectrum.

¹H NMR (500 MHz, Acetone-d6) δ 9.84 (s, 2H), 8.94 (d, J = 2.1 Hz, 2H), 8.58 (dt, J = 8.0, 1.1 Hz, 2H), 8.23 (d, J = 8.0 Hz, 2H), 8.10 (td, J = 7.7, 1.4 Hz, 2H), 7.84 (t, J = 8.0 Hz, 1H), 7.56 (d, J = 2.2 Hz, 2H), 7.52 (dt, J = 5.7, 1.0 Hz, 2H), 7.30 (ddd, J = 7.3, 5.7, 1.4 Hz, 2H), 7.21 (t, J = 7.8 Hz, 2H), 6.92 (d, J = 7.9 Hz, 4H), 0.90 (hept, J = 6.6 Hz, 4H), 0.69 (d, J = 6.6 Hz, 12H), 0.61 (d, J = 6.6 Hz, 12H).

Mass spectrometry: ESI-Mass spectra were recorded by a Waters Synapt 2G (QTOF). HRMS (ESI) m/z 410.681 0.5 [M-2PF₆]²⁺ (calcd for C₄₉H₅₁FeN₉ 821.3617).

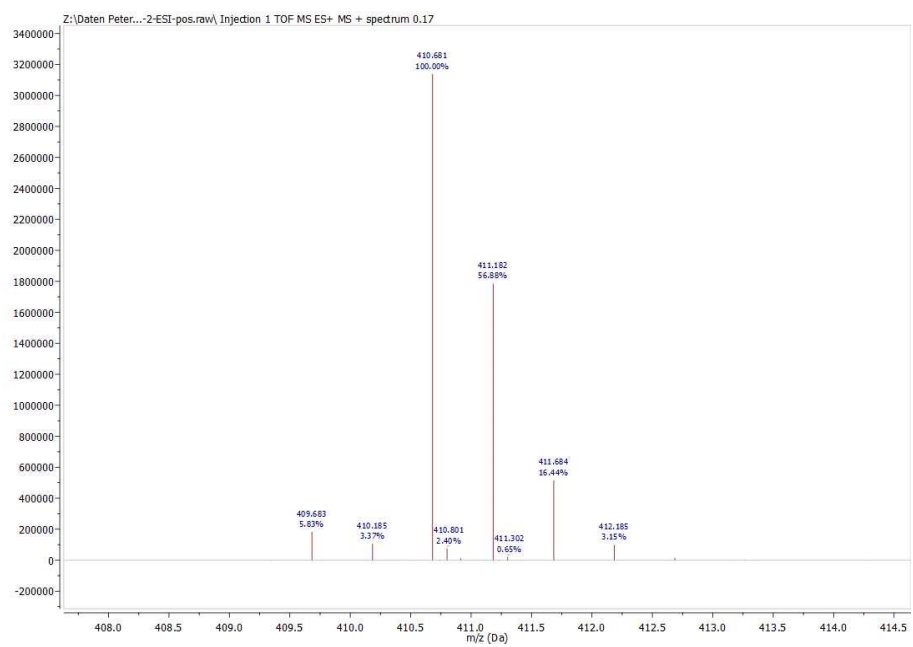


Figure S2: ESI mass spectrum.

S1.2 Optical Absorption Spectrum of [Fe^{II}(tpy)(pyz–NHC)](PF₆)₂

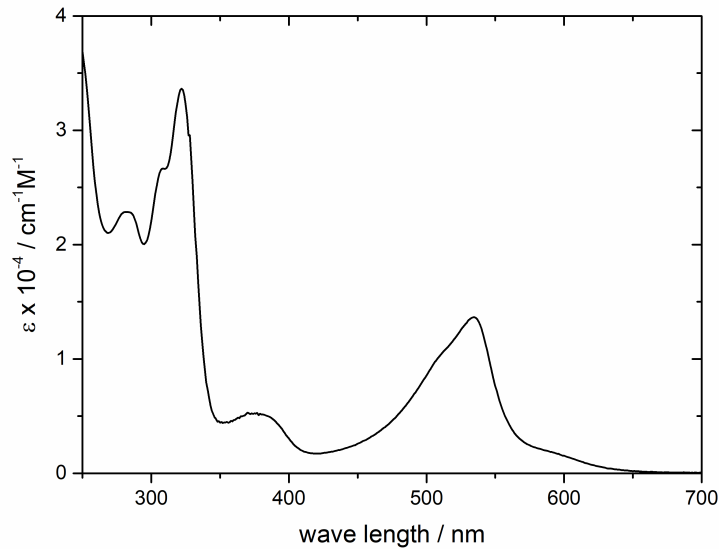


Figure S3: Experimental optical absorption spectrum of [Fe^{II}(tpy)(pyz–NHC)](PF₆)₂ in MeCN.

S1.3 Details of Single Crystal Structure Analysis

Crystal structure data of compound [Fe^{II}(tpy)(pyz–NHC)](PF₆)₂: [C51 H57 F12 Fe N9 O P2], $M = 1157.84$, dark red crystal, $(0.186 \times 0.067 \times 0.042 \text{ mm})$; monoclinic, space group P 21/c; $a = 13.1873(9) \text{ \AA}$, $b = 20.1999(13) \text{ \AA}$, $c = 39.201(3) \text{ \AA}$; $\alpha = 90^\circ$, $\beta = 97.484(4)^\circ$, $\gamma = 90^\circ$, $V = 10353.5(12) \text{ \AA}^3$; $Z = 8$; $\mu = 0.445 \text{ mm}^{-1}$; $\rho_{\text{calc}} = 1.486 \text{ g}\cdot\text{cm}^{-3}$; 140304 reflections ($\vartheta_{\text{max}} = 30.561^\circ$), 30242 unique ($R_{\text{int}} = 0.0833$); 1343 parameters; largest max./min in the final difference Fourier synthesis $3.419 \text{ e}\cdot\text{\AA}^{-3}$ / $-1.226 \text{ e}\cdot\text{\AA}^{-3}$; max./min. transmission $0.75/0.67$; $R_1 = 0.0656$ ($I > 2\sigma(I)$), $wR_2 = 0.1868$ (all data).

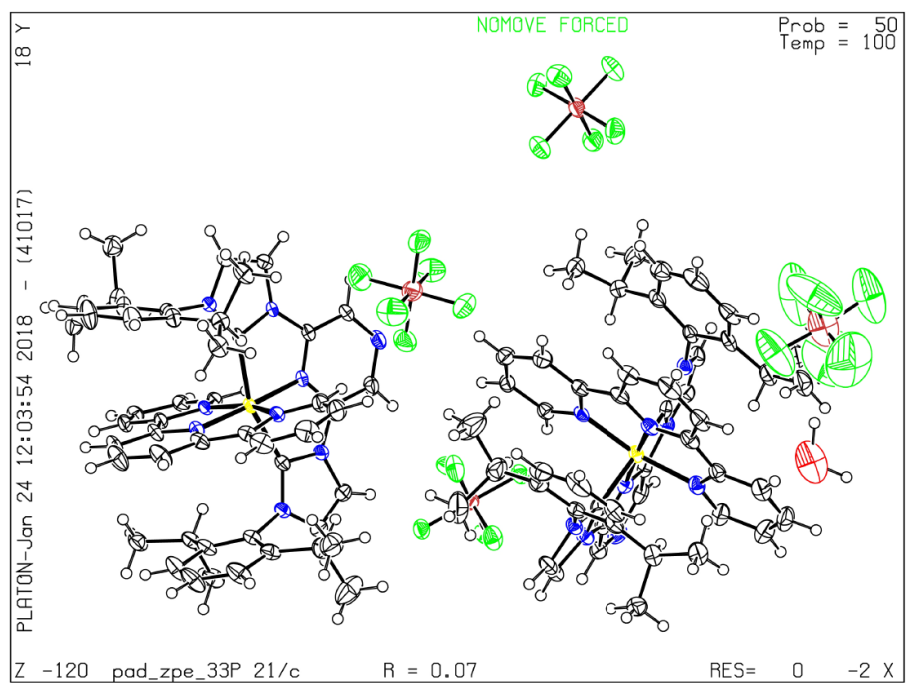


Figure S4: Crystal structure of $[\text{Fe}^{\text{II}}(\text{tpy})(\text{pyz}-\text{NHC})](\text{PF}_6)_2$.

Table S1: Crystal Structure Data.

Identification code	pad_zpe_330m_sq
Empirical formula	C51H57F12FeN9OP2
Formula weight	1157.84
Density (calculated)	1.486 g·cm ⁻³
F(000)	4784
Temperature	100(2) K
Crystal size	0.186 × 0.067 × 0.042 mm
Crystal colour	dark red
Crystal description	prism
Wavelength	0.71073 Å
Crystal system	monoclinic
Space group	<i>P</i> 21/ <i>c</i>
Unit cell dimensions	
a [Å]	13.1873(9)
b [Å]	20.1999(13)
c [Å]	39.201(3)
α [°]	90
β [°]	97.484(4)
γ [°]	90
Volume	10353.5(12) Å ³
Z	8
Cell measurement reflections used	9987
Cell measurement ϑ min/max	2.23°/25.71°
Diffractometer control software	BRUKER D8 KAPPA APEX 2 (3.0-2009)
Diffractometer measurement device	Bruker D8 KAPPA series II with APEX II area detector system

Diffractometer measurement method	Data collection strategy APEX 2/COSMO
ϑ range for data collection	1.855°- 30.561°
Completeness to $\vartheta = 25.242^\circ$	99.3 %
Completeness to $\vartheta_{\max} = 30.561^\circ$	95.2 %
Index ranges	$-18 \leq h \leq 18$ $-28 \leq k \leq 28$ $-55 \leq l \leq 55$
Computing data reduction	BRUKER D8 KAPPA APEX 2 (3.0-2009)
Absorption coefficient	0.445 mm ⁻¹
Absorption correction	Semi-empirical from equivalents
Computation absorption correction	BRUKER AXS SMART APEX 2 Vers. 3.0-2009
Max./min. Transmission	0.75/0.67
R_{merg} before/after correction	0.0600/0.0529
Computing structure solution	BRUKER D8 KAPPA APEX 2 (3.0-2009)
Computing structure refinement	SHELXL-2017/1 (Sheldrick, 2017)
Refinement method	Full-matrix least-squares on F^2
Reflections collected	140304
Independent reflections	30242
R_{int}	0.0833
Reflections with $I > 2\sigma(I)$	14958
Restraints	1
Parameter	1343
GooF	0.999
Weighting details	$w = 1/[\sigma^2(F_{\text{obs}}^2) + (0.0736P)^2 + 13.5191P]$ where $P = (F_{\text{obs}}^2 + 2F_{\text{calc}}^2)/3$
$R_1 [I > 2\sigma(I)]$	0.0656
$wR_2 [I > 2\sigma(I)]$	0.1461

R_1 [all data]	0.1627
wR_2 [all data]	0.1868
Absolute structure parameter	
Largest diff. peak and hole	3.419/-1.226

Table S2: Atomic coordinates ($\times 10^4$) and equivalent isotropic displacement parameters ($\text{\AA}^2 \times 10^3$) for pad_zpe_330m_sq. U_{eq} is defined as one third of the trace of the orthogonalized U_{ij} tensor.

	x	y	z	U_{eq}
O(1)	70(4)	1139(2)	5195(1)	95(2)
H(2)	-634	814	5190	100(20)
H(1)	804	829	5195	67(16)
Fe11	5083(1)	7505(1)	3320(1)	17(1)
N11	4973(2)	8035(1)	2894(1)	19(1)
N21	5475(2)	8338(1)	3510(1)	22(1)
N31	5263(2)	7265(1)	3811(1)	21(1)
N41	4736(2)	6664(1)	3114(1)	18(1)
N51	4243(2)	5436(1)	2827(1)	27(1)
N61	6420(2)	6544(1)	3101(1)	18(1)
N71	7489(2)	7296(1)	3286(1)	19(1)
N81	3117(2)	6946(1)	3150(1)	21(1)
N91	2771(2)	7840(1)	3407(1)	22(1)
C11	4597(2)	7840(2)	2575(1)	21(1)
H11	4369	7396	2541	25
C21	4528(3)	8257(2)	2294(1)	23(1)
H21	4234	8108	2073	28
C31	4897(3)	8901(2)	2340(1)	27(1)
H31	4888	9191	2149	33

C41	5277(3)	9112(2)	2666(1)	25(1)
H41	5523	9552	2702	31
C51	5295(2)	8674(2)	2940(1)	21(1)
C61	5604(3)	8846(2)	3300(1)	24(1)
C71	5979(3)	9452(2)	3432(1)	33(1)
H71	6091	9808	3283	40
C81	6185(3)	9521(2)	3787(1)	42(1)
H81	6436	9931	3883	50
C91	6027(3)	8998(2)	4001(1)	37(1)
H91	6159	9046	4244	44
C101	5673(3)	8402(2)	3855(1)	26(1)
C111	5513(3)	7780(2)	4033(1)	26(1)
C121	5641(3)	7696(2)	4386(1)	36(1)
H121	5790	8065	4534	43
C131	5548(3)	7067(2)	4521(1)	41(1)
H131	5642	6998	4763	49
C141	5317(3)	6544(2)	4299(1)	36(1)
H141	5256	6108	4385	44
C151	5174(3)	6662(2)	3948(1)	28(1)
H151	5006	6299	3797	33
C161	3765(2)	6463(2)	3046(1)	20(1)
C171	3516(3)	5851(2)	2902(1)	26(1)
H171	2819	5723	2856	32
C181	5211(3)	5641(2)	2886(1)	24(1)
H181	5741	5360	2830	29
C191	5455(3)	6257(2)	3029(1)	20(1)
C201	3573(3)	7502(2)	3312(1)	20(1)

C211	2059(3)	6954(2)	3140(1)	28(1)
H211	1586	6631	3042	34
C221	1850(3)	7513(2)	3297(1)	28(1)
H221	1188	7664	3330	34
C231	2884(3)	8418(2)	3628(1)	24(1)
C241	2870(3)	8320(2)	3985(1)	29(1)
C251	3094(3)	8870(2)	4195(1)	40(1)
H251	3100	8827	4436	48
C261	3304(4)	9474(2)	4060(1)	44(1)
H261	3495	9835	4210	53
C271	3241(4)	9563(2)	3708(1)	42(1)
H271	3358	9990	3619	51
C281	3008(3)	9036(2)	3482(1)	28(1)
C291	2559(3)	7669(2)	4136(1)	36(1)
H291	2778	7298	3993	43
C301	1398(4)	7637(3)	4127(1)	65(2)
H30A1	1204	7201	4207	97
H30B1	1069	7710	3891	97
H30C1	1177	7981	4278	97
C311	3014(4)	7556(2)	4510(1)	48(1)
H31A1	2710	7869	4658	72
H31B1	3756	7624	4533	72
H31C1	2869	7102	4577	72
C321	2808(3)	9150(2)	3095(1)	28(1)
H321	3132	8780	2978	33
C331	1648(3)	9133(2)	2976(1)	34(1)
H33A1	1374	8700	3030	51

H33B1	1520	9209	2727	51
H33C1	1311	9480	3095	51
C341	3230(3)	9803(2)	2978(1)	34(1)
H34A1	2858	10172	3066	51
H34B1	3145	9818	2726	51
H34C1	3958	9837	3066	51
C351	6469(2)	7167(2)	3252(1)	19(1)
C361	7362(3)	6304(2)	3043(1)	22(1)
H361	7507	5892	2943	27
C371	8023(3)	6776(2)	3157(1)	23(1)
H371	8741	6761	3152	27
C381	8031(2)	7870(2)	3439(1)	21(1)
C391	8326(3)	7869(2)	3797(1)	25(1)
C401	8934(3)	8392(2)	3932(1)	36(1)
H401	9134	8415	4173	43
C411	9256(3)	8876(2)	3724(1)	44(1)
H411	9688	9222	3822	52
C421	8953(3)	8863(2)	3375(1)	38(1)
H421	9170	9206	3236	45
C431	8334(3)	8357(2)	3220(1)	26(1)
C441	8029(3)	7329(2)	4032(1)	27(1)
H441	7304	7203	3950	32
C451	8077(3)	7553(2)	4407(1)	34(1)
H45A1	7753	7218	4538	51
H45B1	7717	7975	4417	51
H45C1	8793	7607	4507	51
C461	8690(3)	6705(2)	4016(1)	36(1)

H46A1	9397	6804	4112	53
H46B1	8672	6565	3776	53
H46C1	8423	6350	4149	53
C471	8038(3)	8353(2)	2834(1)	27(1)
H471	7399	8086	2781	33
C481	7828(3)	9049(2)	2689(1)	34(1)
H48A1	7419	9296	2838	52
H48B1	7452	9019	2457	52
H48C1	8478	9280	2679	52
C491	8874(3)	8031(2)	2652(1)	39(1)
H49A1	9512	8281	2704	58
H49B1	8662	8032	2403	58
H49C1	8982	7574	2732	58
Fe12	256(1)	3126(1)	3733(1)	20(1)
N12	-743(2)	2615(1)	3960(1)	26(1)
N22	1140(2)	2796(1)	4105(1)	22(1)
N32	1529(2)	3518(1)	3623(1)	20(1)
N42	-714(2)	3448(1)	3368(1)	22(1)
N52	-2262(2)	3854(2)	2872(1)	29(1)
N62	-804(2)	4334(1)	3704(1)	24(1)
N72	168(2)	4428(1)	4182(1)	24(1)
N82	-391(2)	2511(1)	3095(1)	23(1)
N92	845(2)	1889(1)	3302(1)	22(1)
C12	-1738(3)	2519(2)	3850(1)	33(1)
H12	-2033	2741	3648	39
C22	-2350(3)	2111(2)	4017(1)	42(1)
H22	-3050	2054	3929	50

C32	-1942(3)	1789(2)	4312(1)	42(1)
H32	-2353	1503	4428	50
C42	-925(3)	1889(2)	4436(1)	36(1)
H42	-631	1682	4643	43
C52	-337(3)	2296(2)	4253(1)	28(1)
C62	750(3)	2411(2)	4343(1)	28(1)
C72	1396(3)	2170(2)	4626(1)	32(1)
H72	1133	1904	4794	39
C82	2416(3)	2324(2)	4658(1)	36(1)
H82	2862	2160	4849	43
C92	2812(3)	2717(2)	4415(1)	32(1)
H92	3519	2824	4439	38
C102	2141(3)	2949(2)	4136(1)	24(1)
C112	2370(3)	3372(2)	3854(1)	23(1)
C122	3313(3)	3626(2)	3812(1)	30(1)
H122	3894	3516	3972	36
C132	3421(3)	4042(2)	3539(1)	32(1)
H132	4070	4220	3509	38
C142	2561(3)	4193(2)	3309(1)	27(1)
H142	2609	4483	3121	32
C152	1640(3)	3918(2)	3358(1)	23(1)
H152	1056	4016	3197	28
C162	-1206(3)	4020(2)	3400(1)	24(1)
C172	-1980(3)	4223(2)	3150(1)	28(1)
H172	-2316	4632	3178	34
C182	-1777(3)	3285(2)	2838(1)	27(1)
H182	-1969	3017	2641	33

C192	-995(3)	3078(2)	3086(1)	23(1)
C202	-92(3)	3989(2)	3923(1)	22(1)
C212	-978(3)	4965(2)	3829(1)	31(1)
H212	-1434	5290	3722	37
C222	-381(3)	5019(2)	4126(1)	30(1)
H222	-334	5392	4275	36
C232	878(3)	4316(2)	4493(1)	24(1)
C242	1861(3)	4592(2)	4519(1)	34(1)
C252	2488(3)	4498(2)	4831(1)	41(1)
H252	3159	4679	4859	49
C262	2163(3)	4152(2)	5096(1)	45(1)
H262	2609	4094	5304	55
C272	1195(3)	3888(2)	5063(1)	35(1)
H272	982	3648	5250	42
C282	516(3)	3965(2)	4761(1)	26(1)
C292	2231(3)	4992(2)	4234(1)	47(1)
H292	1943	4797	4007	56
C302	3408(4)	5000(3)	4260(2)	84(2)
H30A2	3612	5173	4045	125
H30B2	3672	4549	4299	125
H30C2	3688	5285	4452	125
C312	1934(5)	5725(2)	4240(2)	66(2)
H31A2	2252	5964	4064	100
H31B2	2171	5911	4467	100
H31C2	1189	5767	4192	100
C322	-566(3)	3698(2)	4738(1)	29(1)
H322	-750	3509	4502	35

C332	-697(3)	3152(2)	4996(1)	38(1)
H33A2	-1375	2951	4941	57
H33B2	-631	3340	5229	57
H33C2	-170	2814	4985	57
C342	-1328(3)	4255(2)	4783(1)	36(1)
H34A2	-1326	4576	4595	54
H34B2	-1130	4477	5004	54
H34C2	-2016	4068	4778	54
C352	321(2)	2428(2)	3382(1)	21(1)
C362	-314(3)	2031(2)	2847(1)	28(1)
H362	-726	1988	2631	33
C372	459(3)	1643(2)	2976(1)	26(1)
H372	706	1267	2866	32
C382	1713(3)	1608(2)	3524(1)	24(1)
C392	2694(3)	1764(2)	3454(1)	29(1)
C402	3507(3)	1539(2)	3688(1)	38(1)
H402	4190	1623	3648	45
C412	3326(3)	1193(2)	3978(1)	42(1)
H412	3884	1069	4144	50
C422	2343(3)	1026(2)	4029(1)	36(1)
H422	2238	780	4228	44
C432	1506(3)	1208(2)	3799(1)	29(1)
C442	2897(3)	2146(2)	3137(1)	36(1)
H442	2321	2464	3077	43
C452	3888(4)	2540(2)	3188(1)	54(1)
H45A2	4468	2240	3181	81
H45B2	3953	2764	3412	81

H45C2	3881	2870	3005	81
C462	2944(3)	1692(2)	2829(1)	42(1)
H46A2	3024	1959	2625	63
H46B2	2311	1434	2786	63
H46C2	3528	1391	2877	63
C472	436(3)	963(2)	3830(1)	35(1)
H472	-38	1351	3805	42
C482	82(3)	468(2)	3539(1)	40(1)
H48A2	102	681	3316	60
H48B2	-618	324	3558	60
H48C2	538	82	3559	60
C492	339(4)	622(2)	4174(1)	49(1)
H49A2	-382	523	4188	73
H49B2	604	915	4364	73
H49C2	733	209	4189	73
P13	2521(2)	43(1)	5138(1)	85(1)
F13	2634(4)	818(2)	5199(1)	127(2)
F23	3025(7)	128(3)	4815(1)	192(3)
F33	1480(6)	119(4)	4920(2)	255(4)
F43	3539(5)	-52(2)	5366(1)	167(3)
F53	2008(7)	-16(4)	5460(2)	209(3)
F63	2501(5)	-738(2)	5064(1)	146(2)
P14	6838(1)	1401(1)	3057(1)	29(1)
F14	7007(2)	673(1)	2922(1)	46(1)
F24	6370(2)	1112(1)	3380(1)	47(1)
F34	5719(2)	1414(1)	2837(1)	40(1)
F44	7951(2)	1409(1)	3270(1)	44(1)

F54	7294(2)	1708(1)	2727(1)	38(1)
F64	6654(2)	2140(1)	3188(1)	40(1)
P15	6143(1)	4750(1)	3815(1)	37(1)
F15	6731(2)	5275(1)	3608(1)	58(1)
F25	5125(2)	5179(1)	3720(1)	49(1)
F35	5859(2)	4344(1)	3467(1)	50(1)
F45	6423(2)	5164(2)	4157(1)	67(1)
F55	7157(2)	4321(1)	3905(1)	47(1)
F65	5523(2)	4229(1)	4013(1)	50(1)
P16	-21(1)	5426(1)	2810(1)	23(1)
F16	455(2)	5426(1)	2460(1)	52(1)
F26	-1136(2)	5458(1)	2598(1)	39(1)
F36	-56(2)	4633(1)	2804(1)	29(1)
F46	8(2)	6227(1)	2817(1)	32(1)
F56	1093(2)	5407(1)	3022(1)	51(1)
F66	-513(2)	5436(1)	3160(1)	40(1)

S2 Ground-State Equilibrium Geometry

The ground-state equilibrium geometry of the polypyridyl NHC iron (II) complex as shown in Figure 1 in the main paper was optimized at the LC-BYLP/6-31G* level of theory as described in the Computational Details. The Cartesian coordinates of the resulting geometry are reported in Table S3.

Table S3: Cartesian coordinates of the optimized geometry of the polypyridyl NHC iron (II) complex given in Å.

Atom	x	y	z	Atom	x	y	z
Fe	-0.035763	-0.041454	-0.040577	C	-7.417329	6.747134	3.536045
N	2.431239	0.405669	2.629489	C	-4.325935	6.832579	6.908531
N	0.039456	3.463679	0.010007	C	-6.195464	8.033446	5.489044
N	-2.482305	0.591087	-2.688458	H	-8.888170	7.708529	2.453456
C	1.582753	4.676942	1.669674	H	-3.395140	7.854753	8.442022
C	-1.444886	4.791915	-1.615226	H	-6.729803	9.980861	5.930392
C	1.676989	7.312708	1.750083	C	4.934932	3.014680	-4.420300
C	-1.413996	7.430572	-1.626985	C	3.727235	4.328115	-6.402117
C	0.163824	8.692930	0.078087	C	6.868954	4.087362	-2.926646
H	2.915877	8.271169	3.094480	C	4.480381	6.833651	-6.835774
H	-2.604381	8.481573	-2.945760	C	7.542354	6.600092	-3.443275
H	0.215280	10.755044	0.104029	C	6.369625	7.956187	-5.379050
C	-2.939860	3.096695	-3.199973	H	3.588486	7.910924	-8.354475
C	-4.673463	3.848603	-5.045152	H	9.028199	7.501640	-2.330117
C	-3.755162	-1.172542	-4.031431	H	6.956170	9.897802	-5.777603
C	-5.979093	2.012076	-6.412680	C	-8.296948	2.796477	0.952742
H	-5.001047	5.856502	-5.398994	H	-7.009347	1.434809	0.022221
C	-5.505718	-0.536501	-5.892396	C	-9.405664	4.545361	-1.074146

H	-3.342706	-3.143625	-3.579059	H	-7.982587	5.830337	-1.886018
H	-7.346920	2.565368	-7.854856	H	-10.209837	3.399025	-2.617264
H	-6.479624	-2.040840	-6.911599	H	-10.947152	5.706982	-0.280960
C	2.996639	2.874064	3.209112	C	-10.499033	1.300370	2.143808
C	4.755670	3.499682	5.076686	H	-11.610925	0.368010	0.646848
C	3.620450	-1.447391	3.928018	H	-9.849617	-0.165182	3.466780
C	5.976181	1.571904	6.396376	H	-11.758361	2.604419	3.175067
H	5.168877	5.481100	5.484177	C	-1.720451	2.983539	8.095216
C	5.392552	-0.938818	5.808211	H	-0.732125	1.539742	6.948423
H	3.120819	-3.385619	3.424570	C	-3.036474	1.635218	10.319500
H	7.363389	2.026788	7.854424	H	-1.612225	0.746881	11.555032
H	6.297378	-2.510251	6.789680	H	-4.107494	3.021799	11.451095
H	2.674618	-8.650728	-2.874465	H	-4.352382	0.155004	9.686865
C	-1.715480	-7.559029	1.405337	C	0.256192	4.804116	9.178596
C	-1.680382	-4.923665	1.423071	H	1.100115	6.017279	7.709945
C	1.453089	-4.941097	-1.610922	H	-0.595591	6.044933	10.623507
C	1.417662	-7.576471	-1.636178	H	1.780942	3.717835	10.094564
N	-0.166820	-8.865771	-0.126435	C	8.296250	2.576447	-0.932157
H	-2.996902	-8.620033	2.630106	H	6.965275	1.233375	-0.036169
N	-0.098136	-3.600012	-0.085488	C	9.439009	4.256826	1.133781
C	2.621230	-0.729069	-2.531791	H	11.018511	5.387767	0.371774
C	4.828886	-3.783208	-4.782517	H	8.047004	5.568592	1.956710
C	5.706621	-1.472964	-5.468434	H	10.199262	3.061946	2.662190
H	5.353485	-5.673649	-5.386539	C	10.461833	1.039158	-2.136551
H	7.167604	-0.934186	-6.805035	H	9.776538	-0.393589	-3.477488
C	-2.712365	-0.697037	2.438115	H	11.756963	2.322254	-3.149723
C	-4.993901	-3.728034	4.645626	H	11.545726	0.060485	-0.648384

C	-5.789867	-1.406830	5.391420	C	1.783519	3.080714	-8.119485
H	-5.571818	-5.613497	5.215429	H	0.741469	1.646239	-7.009010
H	-7.218707	-0.851158	6.755389	C	3.080909	1.736293	-10.357558
N	-3.129868	-3.265433	2.850111	H	1.643977	0.906915	-11.618852
N	-4.403196	0.409087	4.039585	H	4.195651	3.114356	-11.456969
N	2.959047	-3.299821	-2.998266	H	4.354722	0.212057	-9.743244
N	4.363411	0.356649	-4.091690	C	-0.128138	4.978120	-9.187640
C	-4.898655	3.075422	4.421718	H	-1.673003	3.953611	-10.140195
C	-6.814623	4.228622	2.964569	H	-0.953102	6.186487	-7.704605
C	-3.642468	4.317324	6.419257	H	0.774869	6.220512	-10.599750

S3 Density of States in the Wigner Ensemble

We show the singlet and triplet density of states (DOS) of the $[\text{Fe}^{\text{II}}(\text{tpy})(\text{pyz}-\text{NHC})]^{2+}$ obtained at the LC-BLYP/6-31G* level of theory for a Wigner ensemble of 200 geometries in Figure S5. As can be seen, the 20 singlet and 20 triplet states cover the energy range up to 3.5 eV. Thus, it is sufficient to include this number of states in the excited-state dynamics simulations.

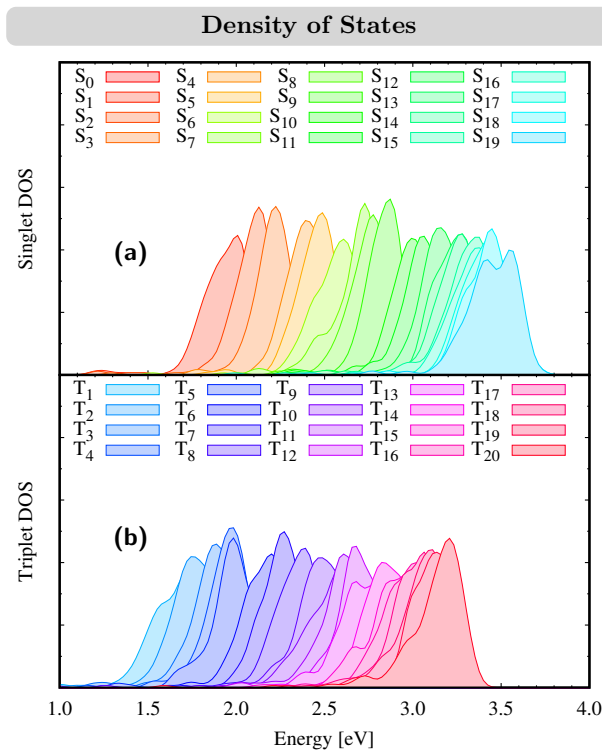


Figure S5: Singlet (a) and triplet (b) density of states of the $[\text{Fe}^{\text{II}}(\text{tpy})(\text{pyz}-\text{NHC})]^{2+}$ obtained at the LC-BLYP/6-31G* level of theory for a Wigner ensemble of 200 geometries.

S4 Excited States at the FC Geometry

The energies, oscillator strengths, as well as state characters of the excited states were computed at the LC-BLYP/6-31G* level of theory at the FC geometry are shown in Table S4

Table S4: Energy in eV, oscillator strength f_{osc} , and excitation character of excited states computed at the FC geometry.

State	Energy	f_{osc}	MC	ML1CT	ML2CT	LMCCT	Lloc	L1L2CT	L2MCT	L2L1loc	L2loc
S_1	1.9988	0.002559	0.0960	0.0260	0.5637	0.0164	0.0045	0.0945	0.0263	0.0066	0.1657
S_2	2.1990	0.007825	0.0657	0.5955	0.0356	0.0129	0.1216	0.0070	0.0149	0.1379	0.0085
S_3	2.2091	0.000006	0.1029	0.0528	0.5806	0.0250	0.0082	0.1485	0.0116	0.0089	0.0611
S_4	2.4478	0.000008	0.0358	0.6573	0.0195	0.0081	0.1353	0.0045	0.0063	0.1296	0.0032
S_5	2.4970	0.000000	0.0838	0.6259	0.0565	0.0082	0.0461	0.0081	0.0179	0.1425	0.0106
S_6	2.6152	0.034548	0.0243	0.6637	0.0102	0.0086	0.2065	0.0035	0.0029	0.0779	0.0019
S_7	2.8017	0.097488	0.0700	0.2985	0.3493	0.0098	0.0780	0.0301	0.0162	0.0505	0.0973
S_8	2.7009	0.000072	0.0385	0.7205	0.0092	0.0042	0.0521	0.0008	0.0075	0.1646	0.0022
S_9	2.8851	0.024686	0.0376	0.2593	0.3985	0.0095	0.0696	0.0635	0.0082	0.0471	0.1062
S_{10}	3.0786	0.000370	0.0583	0.0275	0.6483	0.0119	0.0068	0.1662	0.0079	0.0036	0.0691
S_{11}	3.2355	0.000016	0.4528	0.1745	0.0856	0.0794	0.0306	0.0151	0.1026	0.0405	0.0186
S_{12}	3.2128	0.010524	0.0691	0.0411	0.6193	0.0107	0.0054	0.0450	0.0170	0.0086	0.1834
S_{13}	3.3742	0.000056	0.5069	0.2118	0.0553	0.0331	0.0145	0.0059	0.1127	0.0477	0.0116
S_{14}	3.3798	0.032989	0.0053	0.6129	0.0217	0.0071	0.1760	0.0074	0.0020	0.1612	0.0061
S_{15}	3.4214	0.060784	0.0160	0.4122	0.2639	0.0024	0.0883	0.0410	0.0063	0.1043	0.0651
S_{16}	3.5194	0.014730	0.0049	0.6833	0.0211	0.0019	0.1997	0.0053	0.0009	0.0784	0.0040
S_{17}	3.5521	0.008395	0.0422	0.6149	0.0578	0.0111	0.1736	0.0146	0.0055	0.0701	0.0097
S_{18}	3.6251	0.000685	0.3281	0.2360	0.1295	0.0894	0.0466	0.0267	0.0429	0.0410	0.0593
S_{19}	3.6082	0.000027	0.0053	0.7468	0.0139	0.0004	0.0538	0.0010	0.0012	0.1739	0.0033
T_1	1.6832	0.000000	0.0930	0.0258	0.5638	0.0147	0.0041	0.0896	0.0272	0.0068	0.1746
T_2	1.8402	0.000000	0.0982	0.1493	0.5016	0.0100	0.0390	0.0353	0.0217	0.0192	0.1253
T_3	2.0243	0.000000	0.0733	0.4992	0.1348	0.0172	0.1482	0.0149	0.0117	0.0683	0.0320
T_4	1.9755	0.000000	0.0672	0.5748	0.0577	0.0149	0.1405	0.0091	0.0128	0.1098	0.0129
T_5	1.9117	0.000000	0.1009	0.0657	0.5769	0.0237	0.0085	0.1422	0.0109	0.0117	0.0591
T_6	2.1643	0.000000	0.0466	0.5853	0.0321	0.0107	0.1807	0.0052	0.0095	0.1209	0.0086
T_7	2.3317	0.000000	0.0815	0.6114	0.0738	0.0078	0.0444	0.0133	0.0172	0.1376	0.0125
T_8	2.3245	0.000000	0.0289	0.6344	0.0090	0.0098	0.2322	0.0034	0.0034	0.0773	0.0012
T_9	2.5635	0.000000	0.4869	0.2183	0.0377	0.0777	0.0344	0.0061	0.0900	0.0413	0.0072
T_{10}	2.7368	0.000000	0.4849	0.2359	0.0387	0.1048	0.0470	0.0079	0.0472	0.0274	0.0058
T_{11}	2.7649	0.000000	0.5120	0.2313	0.0376	0.0382	0.0176	0.0032	0.1040	0.0477	0.0080
T_{12}	2.6378	0.000000	0.0318	0.0793	0.5184	0.0046	0.0268	0.0812	0.0111	0.0188	0.2276
T_{13}	2.5457	0.000000	0.0831	0.6619	0.0221	0.0083	0.0489	0.0018	0.0162	0.1500	0.0074
T_{14}	2.9534	0.000000	0.0312	0.0451	0.6239	0.0027	0.0034	0.0440	0.0155	0.0121	0.2216
T_{15}	3.0978	0.000000	0.4606	0.0563	0.2221	0.0733	0.0092	0.0355	0.0876	0.0111	0.0439
T_{16}	2.9337	0.000000	0.0607	0.1090	0.5510	0.0152	0.0401	0.1416	0.0066	0.0152	0.0602
T_{17}	3.1956	0.000000	0.4583	0.0638	0.2323	0.1041	0.0159	0.0529	0.0427	0.0069	0.0229
T_{18}	3.1490	0.000000	0.0095	0.5774	0.0554	0.0032	0.1774	0.0100	0.0020	0.1207	0.0440
T_{19}	3.1812	0.000000	0.0052	0.5818	0.0649	0.0044	0.1855	0.0183	0.0013	0.1290	0.0092
T_{20}	3.3037	0.000000	0.0040	0.1478	0.0050	0.0134	0.7277	0.0108	0.0020	0.0837	0.0051

S5 Normal Modes in LVC Model

Table S5 provides a list of all normal modes and denotes when the modes were excluded in the analysis shown in Figure 5 in the main paper.

Table S5: Normal modes excluded in the LVC model.

No.	ω [cm ⁻¹]	Excluded	No.	ω [cm ⁻¹]	Excluded	No.	ω [cm ⁻¹]	Excluded
7	-15.47	always	115	731.18		223	1344.04	
8	-14.47	always	116	734.21		224	1356.95	
9	18.21	Modes70	117	738.13		225	1357.28	
10	27.33	Modes50	118	750.22		226	1364.43	
11	29.03	Modes40	119	754.02		227	1366.94	
12	30.95	Modes30	120	754.58		228	1368.59	
13	37.10	Modes50	121	761.12		229	1368.63	
14	40.68	Modes30	122	795.55		230	1371.31	
15	46.60	Modes20	123	795.83		231	1386.36	
16	49.83	Modes40	124	796.14		232	1386.46	
17	57.60	Modes40	125	797.96		233	1387.24	
18	58.43	Modes30	126	811.19		234	1387.58	
19	75.19	Modes20	127	811.29		235	1389.26	
20	76.32	Modes10	128	815.83		236	1395.06	
21	82.58	Modes30	129	816.88		237	1410.49	
22	92.92	Modes20	130	832.91		238	1415.49	
23	93.10	Modes30	131	837.38		239	1437.92	
24	106.42	Modes60	132	871.88		240	1448.31	
25	120.78	Modes90	133	873.02		241	1448.46	
26	124.90	Modes100	134	873.06		242	1448.76	
27	126.00	Modes100	135	887.46		243	1448.98	

28	134.16	Modes100	136	888.77		244	1450.44
29	138.01	Modes90	137	888.83		245	1450.63
30	146.51		138	892.79		246	1454.49
31	155.62	Modes100	139	892.84		247	1454.69
32	157.95	Modes80	140	910.39		248	1454.97
33	165.29	Modes40	141	910.48		249	1455.53
34	168.09	Modes20	142	911.31		250	1464.40
35	178.24	Modes30	143	911.44		251	1464.54
36	185.34	Modes20	144	929.49	Modes60	252	1465.67
37	202.47	Modes30	145	935.02	Modes90	253	1466.19
38	211.62	Modes60	146	935.50	Modes80	254	1468.89
39	214.41	Modes60	147	937.18	Modes80	255	1469.25
40	217.07	Modes70	148	937.61	Modes70	256	1475.10
41	223.08	Modes70	149	942.69	Modes60	257	1475.12
42	232.13	Modes60	150	948.79		258	1475.90
43	237.12	Modes60	151	952.28		259	1476.17
44	237.51	Modes70	152	952.62		260	1476.72
45	252.87	Modes90	153	952.94	Modes100	261	1479.84
46	254.80	Modes60	154	953.64	Modes100	262	1479.95
47	261.28	Modes50	155	960.15		263	1501.30
48	266.14	Modes50	156	960.62		264	1501.35
49	282.20	Modes30	157	962.56	Modes100	265	1503.15
50	285.07	Modes50	158	976.47		266	1548.24
51	286.49	Modes80	159	977.05	Modes100	267	1565.28
52	291.21	Modes90	160	997.35	Modes70	268	1576.47
53	297.70	Modes10	161	1015.81	Modes40	269	1578.79
54	299.79	Modes50	162	1018.57	Modes80	270	1580.49

55	303.51	Modes40	163	1033.46	Modes80	271	1586.31
56	305.85	Modes10	164	1037.08		272	1607.80
57	307.28	Modes50	165	1044.74		273	1608.10
58	308.85	Modes50	166	1045.16		274	1612.08
59	310.70	Modes80	167	1050.87		275	1612.17
60	316.29		168	1055.40		276	1614.33 Modes60
61	320.18	Modes50	169	1055.86		277	1625.02
62	331.16	Modes10	170	1056.95		278	1625.12 Modes100
63	333.84	Modes10	171	1064.48		279	1631.24
64	343.33	Modes30	172	1064.87		280	2965.98
65	345.00	Modes30	173	1066.81		281	2966.16
66	354.72	Modes20	174	1077.30		282	2966.60
67	372.08	Modes10	175	1083.75		283	2967.76
68	375.81	Modes20	176	1088.03		284	2980.82
69	395.70	Modes10	177	1089.97		285	2981.09
70	404.59	Modes20	178	1098.52		286	2982.03
71	422.06	Modes20	179	1098.93		287	2982.12
72	433.33	Modes10	180	1106.21		288	2987.65
73	434.35	Modes20	181	1106.40		289	2988.21
74	435.03	Modes10	182	1107.39		290	2988.57
75	444.17	Modes10	183	1112.61		291	2988.65
76	455.37	Modes40	184	1125.20		292	3046.46
77	458.19	Modes40	185	1125.96		293	3046.67
78	460.43	Modes50	186	1129.43		294	3046.87
79	463.18	Modes70	187	1139.08		295	3046.92
80	465.67		188	1140.09		296	3051.84
81	479.73	Modes40	189	1148.61		297	3052.49

82	506.80		190	1148.81		298	3053.66
83	516.55		191	1154.77		299	3053.93
84	516.60	Modes40	192	1159.48		300	3059.77
85	517.48	Modes100	193	1159.50		301	3060.58
86	518.92		194	1169.31		302	3065.21
87	527.19	Modes70	195	1175.53		303	3065.38
88	553.47	Modes90	196	1175.64		304	3081.02
89	553.71	Modes90	197	1176.93		305	3081.68
90	564.83		198	1218.42		306	3084.78
91	566.99		199	1221.00		307	3085.49
92	579.38		200	1253.64		308	3129.15
93	582.87		201	1253.77		309	3129.30
94	598.10		202	1255.71		310	3145.46
95	609.54		203	1256.10		311	3147.33
96	622.56		204	1268.34		312	3148.30
97	624.00		205	1275.49		313	3148.34
98	627.00		206	1277.07		314	3148.38
99	627.08		207	1287.14		315	3149.25
100	633.52	Modes60	208	1291.49		316	3153.00
101	638.01	Modes80	209	1291.79		317	3154.42
102	638.51	Modes90	210	1292.44		318	3154.48
103	639.05	Modes80	211	1293.09		319	3155.91
104	647.03	Modes80	212	1295.25		320	3157.52
105	663.80	Modes70	213	1298.66		321	3157.94
106	670.44		214	1303.85		322	3164.86
107	673.15		215	1307.89		323	3164.88
108	679.24		216	1308.46		324	3170.10

109	695.16		217	1308.84		325	3176.99
110	710.28	Modes90	218	1310.94	Modes90	326	3177.94
111	718.62	Modes70	219	1314.75		327	3231.69
112	724.07		220	1321.31		328	3232.53
113	727.83		221	1323.45		329	3249.36
114	729.73		222	1342.71		330	3250.20

S6 Charge Flow During the Dynamics

In addition to this file, three videos in gif format are provided, that depict the charge flow in terms of atomic hole/electron popultaions of trajectories in singlet states, trajectories in triplet states with small dipole moments, and trajectories in triplet states with large dipole moments, respectively. The corresponding files are named:

- charge_flow_singlet.gif
- charge_flow_triplets_small_dipole_moment.gif
- charge_flow_triplets_large_dipole_moment.gif